Shock wave structure of multi-temperature Grad 10-moment equations for a binary gas mixture

Shock wave structure of multi-temperature Grad 10-moment equations for a binary gas mixture

M. Bisi[1], M. Groppi[1], A. Macaluso[1] and G. Martalò[1]

[1] *Department of Mathematical, Physical and Computer Sciences, University of Parma - Parco Area delle Scienze 53/A, I-43124 Parma, Italy*

PACS 47.40.-x – Compressible flows; Shock waves
PACS 47.45.-n – Rarefied gas dynamics
PACS 47.27.ed – Dynamical systems approaches

Abstract – A multi-temperature formal hydrodynamic limit of kinetic equations, based on Grad type approximation of the distribution functions, is employed for the analysis of the steady shock problem in a binary mixture. The presence of a singular barrier and its effects on the occurrence of either smooth profiles or of weak solutions with a discontinuity is investigated for varying Mach number. Some numerical simulations of mixtures of two noble gases are presented and commented on, with reference also to analogous phenomena in different model descriptions.

Introduction. – Multi-temperature models are being widely used in modeling and investigating inert and reactive mixtures. They can be derived by methods of Extended Thermodynamics [1–3], as well as from kinetic equations by standard Chapman-Enskog asymptotic procedure in the regime of dominant intra-species collisions [4, 5] and by Grad's closures [6, 7].

A multi-temperature description is desirable in several problems of aerothermodynamics [8] and plasma physics [9] at high temperature, especially for gas mixtures whose components have very disparate masses (e.g positive ions and electrons [10]). In such mixtures, sometimes called $\varepsilon-$mixtures [11], energy exchanges between light and heavy components turn out to be slower than the ones within each component or between constituents with comparable masses.

At fluid-dynamic level, this two-scale interaction process is well described by equations involving a large set of variables, which includes the main distinctive macroscopic fields of each component. Therefore, the resulting model is of multi-velocity and multi-temperature type.

Results from Rational Thermodynamics however show that there are some specific physical scenarios in which the relaxation of species mean velocities is faster than for species temperatures [12]. In this paper we consider a single velocity and multi-temperature model to describe a physical situation in which the species velocities have already reached a common value (corresponding to the mean velocity of the whole mixture) while the species temperatures are still well separate. This model is formally obtained starting from a kinetic description, by replacing the distribution functions with suitable Grad approximations [6, 7] and assuming that species velocities share the same value.

We aim at testing such model on the classical problem of shock wave structure. The subject is topical and several interesting results on the occurrence of a smooth solution or on the presence of discontinuities (subshocks) have been proposed [13–17], especially for multi-velocity and multi-temperature Euler-like systems [3, 18, 19] and Grad 10-moment equations [6, 7]. Since fifties [20] it is well known that, even for a single gas, shock wave formation is not accurately described by Navier-Stokes equations, and higher order closures, as Burnett [21] or Grad equations [22], are desirable. The mathematical structure of Grad equations provides the occurrence of non-physical sub-shocks , namely of discontinuous shock wave solutions, for high Mach numbers, and suitable regularizations have been proposed to prevent these effects [23]. For a gas mixture the situation is much more involved, due to the possible presence of more critical values of the system parameters, corresponding to discontinuities in the shock wave profiles [6, 7]. Here, we want to discuss the effects of a single velocity formulation on the shock profiles, by investigating strong and weak solutions and the presence of singular barriers [24] separating the limiting equilibrium

states, and compare them with results obtained for multi-velocity models [6, 7, 18]. The analysis is performed for varying Mach number.
We use typical tools of the qualitative theory of dynamical systems for the construction of both strong and weak solutions, starting from the local stability properties of asymptotic equilibria. Some numerical tests confirm the theoretical results in the case of binary mixtures of noble gases. The role of particle masses is discussed, focusing the attention on overshooting phenomena in temperatures profiles and on the trends of viscous stress tensors, representing the additional Grad corrections to classical Navier-Stokes equations.

The mathematical formulation. – The starting point is a fluid dynamic model for the main macroscopic fields of a binary gas mixture, obtained as formal hydrodynamic limit of a kinetic description. Besides classical Euler and Navier-Stokes closures, Grad provided a suitable approximation of the kinetic distribution function, which led to an alternative closed set of consistent balance equations [25]. More precisely, Grad's closure procedure consists in replacing the species distribution functions in the kinetic description by truncated Hermite polynomial expansions around local Maxwellians, yielding a system of evolution equations for 13 moments of the distribution function of each component: number density n_i, mass velocity $\mathbf{u}_i$, temperature T_i, viscous stress $\boldsymbol{\sigma}_i$ and heat flux $\mathbf{q}_i$ $(i = 1, 2)$. Under suitable hypotheses, such technique can be generalized to derive different fluid dynamic descriptions involving a smaller or greater number of macroscopic fields [26–28].
In particular, in this paper we consider a macroscopic closure which takes into account only moments of the distribution functions up to second order [29, 30]; the resulting 10 moment equations, useful to model the flow in or around micro-electro-mechanical systems [31], can be seen as a proper subsystem of the 13 moment Grad closure, under the assumption of vanishing heat fluxes. Assuming cylindrical symmetry around the $x-$axis for the distribution functions and Maxwell molecules interaction potential, the following one dimensional set of equations for a binary gas mixture is obtained [6]

$$
\begin{aligned}
&\partial_t (n_i) + \partial_x (n_i u_i) = 0\,, \qquad i = 1, 2\\
&\partial_t (m_i n_i u_i) + \partial_x \left(m_i n_i u_i^2 + n_i T_i + \sigma_i\right) = R_i\\
&\partial_t \left(\frac{1}{2} m_i n_i u_i^2 + \frac{3}{2} n_i T_i\right)\\
&\quad + \partial_x \left[\left(\frac{1}{2} m_i n_i u_i^2 + \frac{5}{2} n_i T_i + \sigma_i\right) u_i\right] = S_i + u_i R_i\\
&\partial_t \left(\frac{2}{3} m_i n_i u_i^2 + \sigma_i\right)\\
&\quad + \partial_x \left[\left(\frac{2}{3} m_i n_i u_i^2 + \frac{4}{3} n_i T_i + \frac{7}{3}\sigma_i\right) u_i\right] = V_i + \frac{4}{3} u_i R_i\,,
\end{aligned}
\tag{1}
$$

where t is the time variable, x is the 1-D space variable, m_i is the particle mass and the macroscopic fields are now appropriate scalar functions of space and time variables. The source terms on the right-hand side, describing momentum and energy exchanges between different components, keep trace of the kinetic model and of the interaction potential, and are given by

$$
\begin{aligned}
R_i &= \sum_{j=1}^{2} \nu_{ij}^{(1)} \mu_{ij} n_i n_j \left(u_j - u_i\right)\\
S_i &= 2 n_i \sum_{j=1}^{2} \frac{\nu_{ij}^{(1)} \mu_{ij}}{m_i + m_j} n_j \left[\frac{3}{2}\left(T_j - T_i\right) + \frac{1}{2} m_j \left(u_j - u_i\right)^2\right]\\
V_i &= \sum_{j=1}^{2} \frac{2\nu_{ij}^{(1)} \mu_{ij}}{m_i + m_j} \left[\frac{2}{3} m_j n_j n_i \left(u_j - u_i\right)^2 + n_i \sigma_j - n_j \sigma_i\right]\\
&\quad - \sum_{j=1}^{2} \frac{3\nu_{ij}^{(2)} m_j}{2\left(m_i + m_j\right)^2} \Big[\frac{2}{3} m_j n_j m_i n_i \left(u_j - u_i\right)^2\\
&\qquad + m_i n_i \sigma_j + m_j n_j \sigma_i\Big]\,,
\end{aligned}
\tag{2}
$$

where $\mu_{ij} = m_i m_j/(m_i + m_j)$ is the reduced mass and $\nu_{ij}^{(k)}$, $i, j, k = 1, 2$, which represent moments of order 1 and 2 of the collision frequencies appearing in Boltzmann operators, are constant in the case of Maxwell molecule interaction potential (with the natural simmetry property $\nu_{12}^{(k)} = \nu_{21}^{(k)}$, $k = 1, 2$). Contributions R_i, S_i, V_i have been computed as suitable moments of bi-species Boltzmann collision operators, using Grad approximation for distribution functions.
Here, we reduce to the case of a single velocity model, assuming that species velocities share the same value ($u_1 = u_2 = u$, where u is the mixture mean velocity). We obtain a set of 7 independent equations, that may be cast in an equivalent way as

$$
\begin{aligned}
&\partial_t (n_1) + \partial_x (n_1 u) = 0\\
&\partial_t (n_2) + \partial_x (n_2 u) = 0\\
&\partial_t (\rho u) + \partial_x \left(\rho u^2 + nT + \sigma\right) = 0\\
&\partial_t \left(\frac{1}{2}\rho u^2 + \frac{3}{2} nT\right)\\
&\qquad + \partial_x \left[\left(\frac{1}{2}\rho u^2 + \frac{5}{2} nT + \sigma\right) u\right] = 0\\
&\partial_t \left(\frac{1}{2} m_1 n_1 u^2 + \frac{3}{2} n_1 T_1\right)\\
&\qquad + \partial_x \left[\left(\frac{1}{2} m_1 n_1 u^2 + \frac{5}{2} n_1 T_1 + \sigma_1\right) u\right] = S_1\\
&\partial_t \left(\frac{2}{3} m_i n_i u^2 + \sigma_i\right)\\
&\quad + \partial_x \left[\left(\frac{2}{3} m_i n_i u^2 + \frac{4}{3} n_i T_i + \frac{7}{3}\sigma_i\right) u\right] = V_i\,, i = 1, 2\,,
\end{aligned}
\tag{3}
$$

where global macroscopic fields can be expressed in terms of species variables as follows

$$\begin{aligned} n = n_1 + n_2 \,, \qquad \rho = \rho_1 + \rho_2 = m_1 n_1 + m_2 n_2 \\ nT = n_1 T_1 + n_2 T_2 \,, \qquad \sigma = \sigma_1 + \sigma_2 \,, \end{aligned} \tag{4}$$

and the source terms reduce to

$$\begin{aligned} S_1 &= 3 \frac{\nu_{12}^{(1)}}{(m_1+m_2)^2} \rho_1 \rho_2 \left(T_2 - T_1\right) \\ V_i &= \kappa_{ji} \Big[2\nu_{ij}^{(1)} \kappa_{ij} \left(n_i \sigma_j - n_j \sigma_i\right) \\ &\quad - \frac{3}{2} \nu_{ij}^{(2)} \left(\kappa_{ij} n_i \sigma_j + \kappa_{ji} n_j \sigma_i\right) \Big] - \frac{3}{4} \nu_{ii}^{(2)} n_i \sigma_i \,, \end{aligned} \tag{5}$$

where $i, j = 1, 2$, $i \neq j$, and $\kappa_{ij} = m_i/(m_i + m_j)$ is the mass ratio.
The steady shock wave problem consists in finding the space-dependent solution

$$\bar{\boldsymbol{\omega}}(x) = (n_1(x), n_2(x), u(x), T_1(x), T_2(x), \sigma_1(x), \sigma_2(x)) \tag{6}$$

of the steady version of (3)

$$\begin{aligned} &\frac{d}{dx}\left(n_1 u\right) = 0 \\ &\frac{d}{dx}\left(n_2 u\right) = 0 \\ &\frac{d}{dx}\left(\rho u^2 + nT + \sigma\right) = 0 \\ &\frac{d}{dx}\left[\left(\frac{1}{2}\rho u^2 + \frac{5}{2} nT + \sigma\right) u\right] = 0 \\ &\frac{d}{dx}\left[\left(\frac{1}{2} m_1 n_1 u^2 + \frac{5}{2} n_1 T_1 + \sigma_1\right) u\right] = S_1 \\ &\frac{d}{dx}\left[\left(\frac{2}{3} m_i n_i u^2 + \frac{4}{3} n_i T_i + \frac{7}{3}\sigma_i\right) u\right] = V_i \,, i = 1, 2 \,, \end{aligned} \tag{7}$$

such that

$$\lim_{x \longrightarrow \pm\infty} \bar{\boldsymbol{\omega}}(x) = \bar{\boldsymbol{\omega}}_\pm \,, \qquad \lim_{x \longrightarrow \pm\infty} \frac{d\bar{\boldsymbol{\omega}}}{dx}(x) = \mathbf{0} \,, \tag{8}$$

where $\bar{\boldsymbol{\omega}}_\pm$ are two given equilibria of the system (7) (correspondingly, at the kinetic level they would give the macroscopic moments of the equilibrium Maxwellians at $\pm\infty$). Equilibria are characterized by a common value of the species temperatures, coinciding with the mixture temperature from (4), and vanishing viscous stresses, i.e.

$$\bar{\boldsymbol{\omega}} = (n_{1,\pm}, n_{2,\pm}, u_\pm, T_\pm, T_\pm, 0, 0) \,. \tag{9}$$

The two equilibria satisfy the Rankine-Hugoniot conditions of the equilibrium subsystem, which consists in a set of conservation equations and coincides with the Euler equations for a mixture as a whole. More precisely, we have [32]

$$\begin{aligned} n_{i+} = \frac{4M^2}{M^2+3} n_{i-} \,, \; i = 1, 2 \,, \quad u_+ = \frac{M^2+3}{4M^2} u_- \\ T_+ = \frac{(M^2+3)(5M^2-1)}{16M^2} T_- \,, \end{aligned} \tag{10}$$

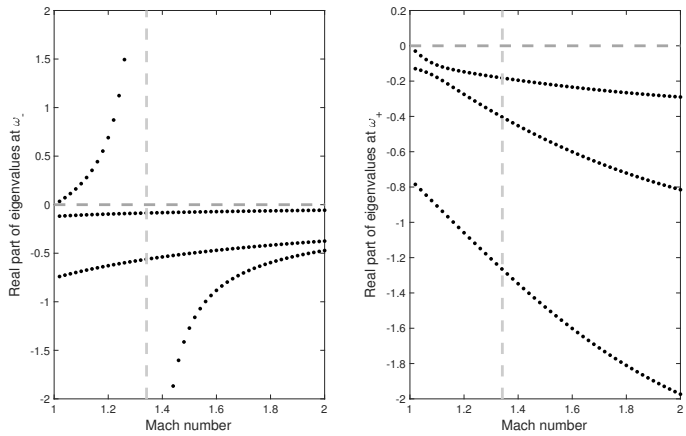

Fig. 1: Eigenvalues of the Jacobian matrix associated to (23) versus Mach number evaluated at $\boldsymbol{\omega} = \boldsymbol{\omega}_-$ (left panel) and at $\boldsymbol{\omega} = \boldsymbol{\omega}_+$ (right panel) for the mixture of the reference case (25).

where $M = \sqrt{3\rho_- u_-^2/(5 n_- T_-)}$ is the Mach number evaluated at $-\infty$, and we consider the supersonic regime $M > 1$.

Shock wave solutions. – We can rewrite the system (7) by using the conservation equations to express part of the macroscopic fields in terms of the remaining ones. In particular, after a suitable change of variables

$$(T_1, T_2) \longrightarrow (T, \theta) = \left(\frac{n_1 T_1 + n_2 T_2}{n}, T_2 - T_1\right) \,, \tag{11}$$

we consider $\boldsymbol{\omega} = (u, \theta, \sigma_2)$ as the set of independent variables; the other macroscopic fields are given by

$$\begin{aligned} n_1 &= \frac{J_1}{u} \,, \qquad n_2 = \frac{J_2}{u} \\ T &= \frac{2}{3} \frac{J_4 - J_3 u}{J_1 + J_2} + \frac{1}{3} \frac{m_1 J_1 + m_2 J_2}{J_1 + J_2} u^2 \\ \sigma_1 &= -\frac{2J_4 - 5J_3 u}{3u} - \frac{4}{3}(m_1 J_1 + m_2 J_2) u - \sigma_2 \,, \end{aligned} \tag{12}$$

where

$$\begin{aligned} J_1 &= n_{1-} u_- \,, \qquad J_2 = n_{2-} u_- \\ J_3 &= \rho_- u_-^2 + n_- T_- \\ J_4 &= \left[\frac{1}{2}\rho_- u_-^2 + \frac{5}{2} n_- T_-\right] u_- \,. \end{aligned} \tag{13}$$

The system (7) can be rewritten in compact form as

$$\mathbf{A} \frac{d\boldsymbol{\omega}}{dx} = \mathbf{G} \,, \tag{14}$$

where $\mathbf{G} = (S_1, V_1, V_2)$, with S_1, V_1 and V_2 expressed in terms of $\boldsymbol{\omega}$; the entries of the matrix $\mathbf{A} = \mathbf{A}(\boldsymbol{\omega})$ are not reported here for brevity.
Some algebra allows to compute the determinant

$$\det(\mathbf{A}) = \frac{9}{2} \frac{J_1 J_2}{n} \left[-\rho u^2 + 3\left(nT + \sigma\right)\right] \,, \tag{15}$$

whose sign obviously depends on the sign of

$$\mathcal{B}(\boldsymbol{\omega}) = -\rho u^2 + 3(nT + \sigma)\,, \tag{16}$$

which individuates the so-called *singular barrier*. Geometrically, in the space Ω spanned by (u, θ, σ_2), this term determines a surface Ω_0 defined by $\mathcal{B}(\boldsymbol{\omega}) = 0$ and a partition

$$\Omega = \Omega_- \cup \Omega_0 \cup \Omega_+\,, \tag{17}$$

where

$$\Omega_\pm = \{\boldsymbol{\omega} \in \Omega \,|\, \mathcal{B}(\boldsymbol{\omega}) \gtrless 0\}\,. \tag{18}$$

We can observe that

$$\mathcal{B}(\boldsymbol{\omega}_-) = -\frac{5}{3} n_- T_- \left(M^2 - \frac{9}{5}\right) \gtrless 0 \text{ iff } M \lessgtr \sqrt{\frac{9}{5}}\,,$$

$$\mathcal{B}(\boldsymbol{\omega}_+) = \frac{10}{3} n_- T_- \left(M^2 - \frac{3}{5}\right) > 0 \qquad \forall M > 1\,,$$

or, equivalently,

$$\boldsymbol{\omega}_- \in \Omega_\pm \text{ if and only if } M \lessgtr \sqrt{\frac{9}{5}}\,,$$

$$\boldsymbol{\omega}_+ \in \Omega_+ \qquad \forall M > 1\,.$$

It is easy to notice that, when $M > \sqrt{9/5}$, the two asymptotic states belong to different subsets of Ω ($\boldsymbol{\omega}_- \in \Omega_-$, $\boldsymbol{\omega}_+ \in \Omega_+$). In this case, we cannot connect the two states at $\pm\infty$ by a continuous profile, since it should cross Ω_0 at least in a point (and hence a singularity should intervene). When $M < \sqrt{9/5}$, both equilibria belong to Ω_+; in this case, a continuous solution could be obtained connecting the two limiting configurations.
The critical Mach number $M^* = \sqrt{9/5}$ corresponds to the critical value

$$u^* = \frac{3}{4}\,\frac{J_3}{m_1 J_1 + m_2 J_2} \tag{19}$$

for the mean velocity u, and we can observe that

$$u_+ < u_- < u^* \text{ for } M < M^*\,;$$

$$u_+ < u^* < u_- \text{ for } M > M^*\,.$$

As already observed above, when $M > M^*$, the solution for u cannot be continuous due to the singularity occurring for $u = u^*$.
When a discontinuity occurs for $M > M^*$, we look for a weak piecewise smooth solution with a jump in some point x_0, fulfilling equations (7). We notice that, since the right-hand side contributions in the balance equations in (7) are bounded functions, those equations imply the continuity of the terms under derivative operator across the jump. It follows that we can express the configuration on the right side of the jump $\boldsymbol{\omega}_R = (u_R, \theta_R, \sigma_{2R})$ in terms of the state on the left side $\boldsymbol{\omega}_L = (u_L, \theta_L, \sigma_{2L})$; in particular, there are two possible outputs for the right side configuration: the continuous solution $\boldsymbol{\omega}_R = \boldsymbol{\omega}_L$ and the discontinuous one given by

$$\begin{aligned} u_R &= \frac{3}{2}\,\frac{J_3}{m_1 J_1 + m_2 J_2} - u_L \\ \theta_R &= \theta_L + \frac{1}{6}\,\frac{m_2 - m_1}{m_1 J_1 + m_2 J_2}\, J_3 (u_L - u_R) \\ \sigma_{2R} &= \sigma_{2L}\frac{u_L}{u_R} + \frac{1}{3}\,\frac{m_2 J_2 J_3}{m_1 J_1 + m_2 J_2}\left(\frac{u_L}{u_R} - 1\right)\,; \end{aligned} \tag{20}$$

we notice that the temperature difference does not have a discontinuity if the two components share the same mass. We can observe also that across the jump

$$\mathcal{B}(\boldsymbol{\omega}_R) = -\mathcal{B}(\boldsymbol{\omega}_L)\,, \tag{21}$$

hence the two states at left and right side of the jump, belonging to disjoint components of the partition (17), are characterized by the same magnitude of the term $\mathcal{B}$.
In the particular case in which $\boldsymbol{\omega}_L = \boldsymbol{\omega}_-$, it is possible to rewrite conditions (20) in terms of the asymptotic state and of the Mach number as follows

$$\begin{aligned} u_R &= \frac{5M^2 + 9}{10M^2} u_- < u_- \\ \theta_R &= \frac{1}{6}(m_2 - m_1)\frac{5M^2 + 3}{5M^2}\,\frac{5M^2 - 9}{10M^2} u_-^2 > 0 \\ \sigma_{2R} &= \frac{1}{3}\,\frac{5M^2 + 3}{5M^2}\,\frac{5M^2 - 9}{5M^2 + 9}\,\rho_{2-} u_-^2 > 0\,. \end{aligned} \tag{22}$$

We remark also that the unique critical value of Mach number involves macroscopic fields of both components, whose profiles exhibit a discontinuity at the same point x_0; this follows from the single velocity structure of equations. In fact, if we considered the complete structure (1) with both species mean velocities, then we would observe the presence of two critical values for the Mach number and the occurrence of two separate singular barriers, which introduce up to two separate discontinuities in the shock profile, each of them involving only the macroscopic moments of one of the two gas components. Moreover, when the Mach number is between the two critical values, macroscopic quantities of a species would have a continuous profile, while those of the other constituent would be discontinuous [6].

Numerical results. – The system (7) can be rewritten in the normal form $d\boldsymbol{\omega}/dx = \mathbf{A}^{-1}\mathbf{G}$, namely

$$\begin{aligned} \frac{du}{dx} &= \frac{V_1 + V_2}{\mathcal{B}} \\ \frac{d\theta}{dx} &= -\frac{14}{27}\,\frac{n}{n_1 n_2 u} S_1 + \frac{2}{9}\,\frac{n}{n_1 n_2 u \mathcal{B}}(V_1 \mathcal{B}_2 - V_2 \mathcal{B}_1) \\ \frac{d\sigma_2}{dx} &= \frac{8}{27u} S_1 + \frac{5}{9u} V_2 - \frac{V_1 + V_2}{u\mathcal{B}}\left(\sigma_2 + \frac{4}{9}\rho_2 u^2\right)\,, \end{aligned} \tag{23}$$

when the matrix $\mathbf{A}$ is not singular, i.e. in any subset of the $x-$line where the solution is regular. Terms

$$\mathcal{B}_i(\boldsymbol{\omega}) = -\rho_i u^2 + 3\frac{n_i}{n}(nT + \sigma)\,, \qquad i = 1, 2\,, \tag{24}$$

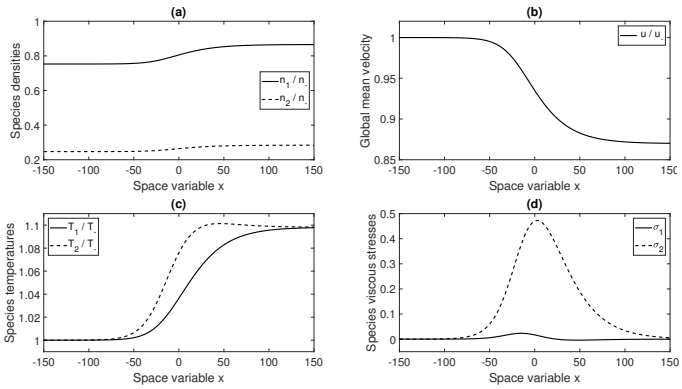

Fig. 2: Profiles of normalized species densities (panel (a)), global mean velocity (panel (b)), species temperatures (panel (c)) and species viscous stresses (panel (d)) versus space variable x in the reference case (25) when $M = 1.1$.

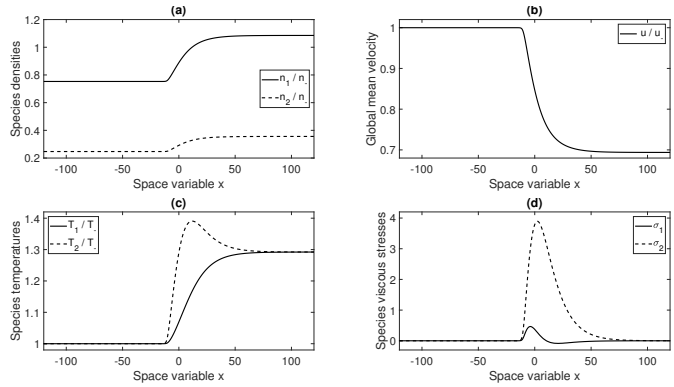

Fig. 3: Profiles of normalized species densities (panel (a)), global mean velocity (panel (b)), species temperatures (panel (c)) and species viscous stresses (panel (d)) versus space variable x in the reference case (25) when $M = 1.3$.

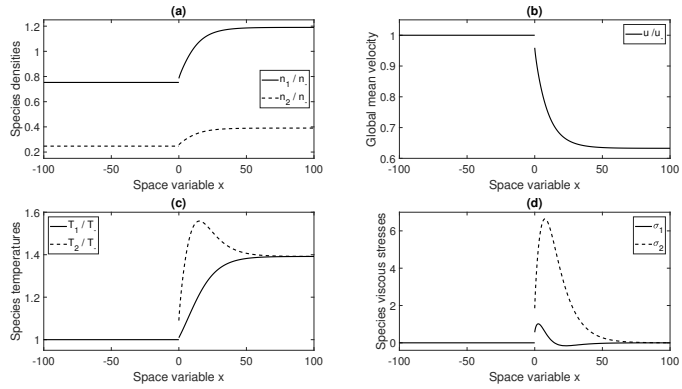

Fig. 4: Profiles of normalized species densities (panel (a)), global mean velocity (panel (b)), species temperatures (panel (c)) and species viscous stresses (panel (d)) versus space variable x in the reference case (25) when $M = 1.4$.

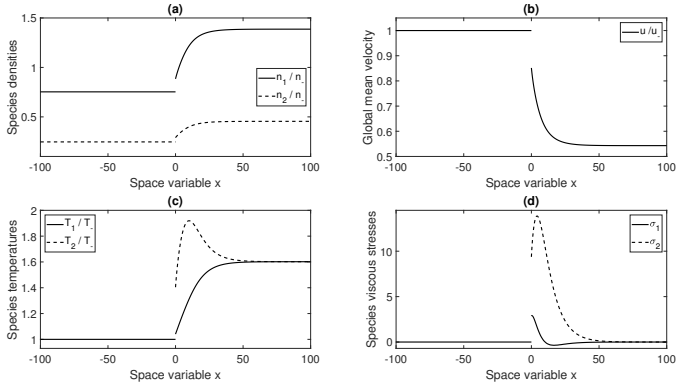

Fig. 5: Profiles of normalized species densities (panel (a)), global mean velocity (panel (b)), species temperatures (panel (c)) and species viscous stresses (panel (d)) versus space variable x in the reference case (25) when $M = 1.6$.

are such that $\mathcal{B} = \mathcal{B}_1 + \mathcal{B}_2$.

For such system, we use typical tools of the qualitative theory of dynamical systems to build up the shock solution in mixtures of noble gases. More precisely, we investigate numerically the stability of asymptotic equilibria and get some information about their stable and unstable manifolds.

We fix a reference case [2, 18] by considering a mixture of Helium (species 1) and Argon (species 2) ($m_1 < m_2$, $m_1/m_2 \simeq 0.1002$) at $40°C$ with concentrations at $-\infty$

$$n_{1-}/n_- = 0.753\,, \qquad n_{2-}/n_- = 0.247\,, \tag{25}$$

respectively, and mean velocity at $-\infty$ obtained by the definition of Mach number ($u_- = \sqrt{5n_-T_-M^2/(3\rho_-)}$).

The constant collision frequencies are obtained by following the approach proposed in [33] and using the numerical values given in [34] for the considered mixture; in particular, we fix the non-dimensional frequencies as follows

$$\begin{aligned} \nu_{11}^{(1)} &= 2.3635\,, \quad \nu_{22}^{(1)} = 2.0501\,, \quad \nu_{12}^{(1)} = 1.7770 \\ \nu_{11}^{(2)} &= 1.8908\,, \quad \nu_{22}^{(2)} = 1.6401\,, \quad \nu_{12}^{(2)} = 1.4216\,. \end{aligned} \tag{26}$$

As shown in Figure 1 (left panel), when $M < M^*$ the Jacobian matrix associated to (23) evaluated at $-\infty$ has two negative eigenvalues and one positive eigenvalue, that diverges to ∞ as $M \longrightarrow M^*$. Therefore, the equilibrium $\boldsymbol{\omega}_-$ is a saddle; the unstable and stable manifolds have dimension 1 and 2, respectively.

When $M > M^*$, the equilibrium is asymptotically stable, since all the eigenvalues are negative; the stable manifold has dimension 3 and no unstable manifold is present.

As concerns the equilibrium $\boldsymbol{\omega}_+$, it is asymptotically stable for any $M > 1$ and the stable manifold has dimension 3 (see the right panel of Figure 1).

When $M < M^*$, it is possible to connect the saddle $\boldsymbol{\omega}_-$ to the asymptotically stable equilibrium $\boldsymbol{\omega}_+$ through a heteroclinic orbit, obtained following the one dimensional unstable manifold tangent to the one dimensional unstable

eigenspace at $-\infty$. This smooth trajectory connecting the two limiting configurations in our study case is shown in Figures 2 and 3 for $M = 1.1, 1.3$, respectively (the profiles are normalized with respect to the equilibrium values n_-, u_-, T_- and translated to have $u(0) = (u_- + u_+)/2$).
When $M > M^*$, both equilibria are asymptotically stable; then no smooth heteroclinic orbit between the two asymptotic states is allowed. The only admissible shock profile is a weak solution. In particular, the only way to satisfy the limiting condition at $-\infty$ is to consider a constant solution $\boldsymbol{\omega} = \boldsymbol{\omega}_-$; then a jump, fulfilling conditions (22), intervenes and the smooth trajectory starting from $\boldsymbol{\omega}_R$ is asymptotically attracted by $\boldsymbol{\omega}_+$ (see Figures 4 and 5 for $M = 1.4, 1.6$, respectively). The profiles are plotted with the discontinuity at $x = 0$.
We can observe that, for increasing Mach number, the transition from the stationary point $\boldsymbol{\omega}_-$ to the equilibrium $\boldsymbol{\omega}_+$ is more and more steep, and the shock profiles for mean velocity and species temperature exhibit a fast decrease/increase, respectively (see for example panels (b) and (c) in Figure 3). This rapid transition implies a very evident overshooting of the heaviest species temperature, already slightly present for $M = 1.1$ (see panel (c) in Figure 2), and a more significant deviation from vanishing viscous stress for such component (see also panel (d) in Figure 3). This behavior is more and more evident for high values of the Mach number, both for temperature and viscous stress (see panels (c) and (d) in Figures 4 and 5). In this analysis, a key role is played by the ratio of particle masses $m_1/m_2 < 1$, especially for what regards the temperature overshooting and the deviation of viscous stress from the null equilibrium value.
We consider now two different mixtures of noble gases: the first one is composed by Neon and Argon with particle masses of the same order ($m_1/m_2 \simeq 0.5051$); the second one is a mixture of Helium and Xenon, and hence with very disparate masses ($m_1/m_2 \simeq 0.0305$).
In both cases, as well as in the case of a mixture of Helium and Argon, the eigenvalues of the jacobian matrix in the limiting configurations are real and the stable and unstable manifolds have the same dimension as above. One of the main differences concerns the behavior of species temperatures; in fact, when masses are of the same order, species temperature profiles do not reach values significantly higher than the equilibrium value T_+ at $+\infty$ (we only observe a slight overshooting of the second component temperature for $M = 1.6$ in Figure 6 top right); moreover, the two profiles are closer to each other than in the reference case (see first row in Figure 6), suggesting that a hydrodynamic description involving only the mixture temperature in this case could be sufficiently accurate to approximate the behavior of both components. In the limit case $m_1/m_2 = 1$ the case of a single gas can be reproduced, since the two identical components share the same profile of mean velocity and temperature, which coincide with the profiles of global quantities.
When particle masses are very disparate, the temperature

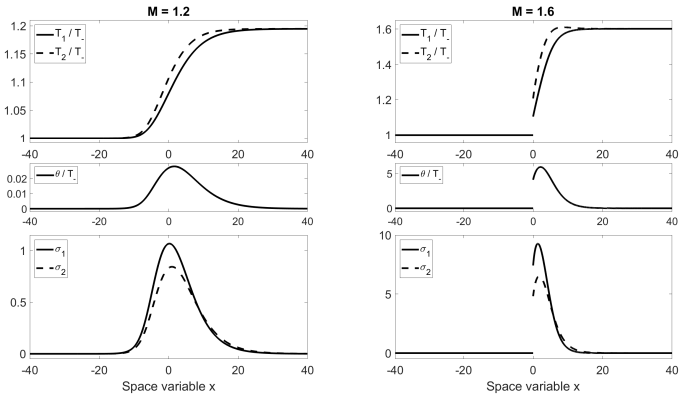

Fig. 6: Profiles of normalized species temperatures (first row), temperature difference (second row) and viscous stresses (third row) for a mixture of Neon and Argon for $M = 1.3$ (left column) and $M = 1.6$ (right column).

overshooting is more evident (see first row in Figure 7). In this case, a multi-temperature description is more suited to well catch the discrepancy between components, since the profile of the mixture temperature could not approximate accurately the species ones.
As concerns the viscous stress, we can notice that the deviation from the null equilibrium value is strictly related to temperatures behavior, and the maximum is reached in correspondence of the highest value of temperature difference (see second and third rows in Figures 6 and 7). Moreover, when component masses are comparable, the two species viscous stresses are of the same order of magnitude, while the stress of the heavy constituent is significantly higher than the light species one when masses are very disparate.

Conclusions. – In this work we investigated the shock wave structure solution in a Grad 10-moment model with a single velocity.
We have observed that the assumption of a common value for species velocities leads to a different scenario, with respect to the one involving multi-velocity equations [6]. The absence of momentum exchanges and the presence of energy exchanges due to thermal effects imply only a partial distinction between components; in fact, the species singular barriers of multi-velocity and multi-temperature models [3,6,7,18] here relax to a single barrier, depending on global macroscopic fields (density, mean velocity, temperature and viscous stress of the mixture as a whole).
The role of the singular barrier Ω_0, which introduces a proper partition of the physical space Ω, has been explicitly analyzed. If the limiting asymptotic equilibria $\boldsymbol{\omega}_\pm$ belong to disjoint subsets of Ω, then only a piecewise smooth solution can connect the two states and an appropriate discontinuity fulfilling the balance equations appears. On the other hand, when $\boldsymbol{\omega}_\pm$ belong to the same subset (in particular $\boldsymbol{\omega}_\pm \in \Omega_+$), then a classical smooth solution can be built up, and $\boldsymbol{\omega}_+$ can be reached asymptotically from

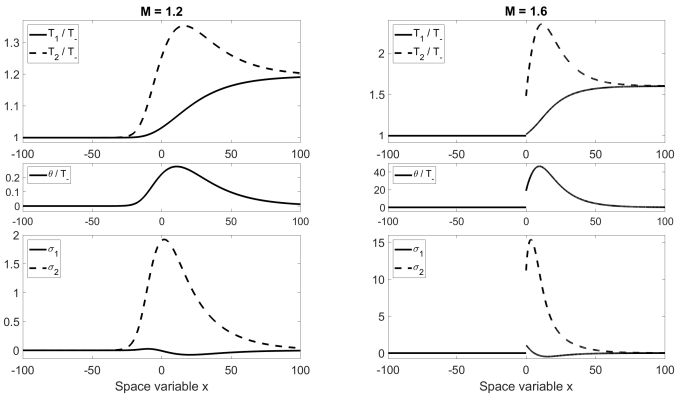

Fig. 7: Profiles of normalized species temperatures (first row), temperature difference (second row) and viscous stresses (third row) for a mixture of Helium and Xenon for $M = 1.3$ (left column) and $M = 1.6$ (right column).

$\boldsymbol{\omega}_-$ moving along the heteroclinic orbit connecting the two equilibria in the phase space.
The theoretical results have been confirmed by simulating binary mixtures of noble gases. The role of particle mass ratio m_1/m_2 has been discussed, by remarking the very evident temperature overshooting when particle masses are very disparate, as well as the different order of magnitude of species viscous stresses, and suggesting again the necessity of a large set of hydrodynamic fields in presence of $\varepsilon-$mixtures of heavy and light components [11]. On the contrary, when masses are comparable, temperature profiles do not overshoot the equilibrium value T_+ and the species macroscopic quantities are very close to each other, suggesting that a single temperature model is sufficiently accurate to describe the shock wave structure problem.
Finally, it is worth noting that the occurrence of temperature overshooting phenomena has been observed experimentally in shock wave formation and combustion problems [2, 35, 36].

* * *

This work was performed in the frame of activities sponsored by the Italian National Group of Mathematical Physics (GNFM-INdAM) and by the University of Parma (Italy), and supported by the Italian National Research Project *Multiscale phenomena in Continuum Mechanics: singular limits, off-equilibrium and transitions* (Prin 2017YBKNCE).

REFERENCES

[1] Ruggeri T. and Simic S., *Math Method. Appl. Sci.*, **30** (2007) 827-849.
[2] Madjarevic D. and Simic S., *EPL*, **102** (2013) 44002.
[3] Conforto F., Mentrelli A. and Ruggeri T., *Ric. di Mat.*, **66** (2017) 221-231.
[4] Bisi M., Martalò G. and Spiga G., *EPL*, **95** (2011) 55002.
[5] Bisi M., Groppi M. and Martalò G. , *J. Phys. A: Math. Theor.*, **-** (2021) 1-19. DOI: https://doi.org/10.1088/1751-8121/abbd1b.
[6] Bisi M., Conforto F. and Martalò G., *Continuum Mech. Therm.*, **28** (2016) 1295-1324.
[7] Artale V., Conforto F. Martalò G. and Ricciardello A., *Ric. di Mat.*, **68** (2019) 485-502.
[8] Bose T. K., *High Temperature Gas Dynamics* (Springer, Berlin) 2003.
[9] Ramshaw J. D., *J. Non-Equilib. Thermodyn.*, **18** (1993) 121-134.
[10] Klingenberg C., Pirner M. and Puppo G., *Kinet. Relat. Mod.*, **10** (2017) 445-465.
[11] Galkin V. S. and Makashev N. K., *Fluid Dyn.*, **29** (1994) 140-155.
[12] Ruggeri T. and Simic S., *Phys. Rev. E*, **80** (2009) 026317.
[13] Alì G. and Romano V., *J. Math. Phys.*, **35** (1994) 2878-2901.
[14] Becker P. A. and Kazanas T., *Astrophys. J.*, **546** (2001) 429-446.
[15] Lee L. C. and Wu B. H., *Geophys. Res. Lett.*, **28** (2001) 1119-1122.
[16] Taniguchi S. and Ruggeri T., *Int. J. Non-Linear Mech.*, **99** (2018) 69-78.
[17] Simic S., *Nonlinearity*, **22** (2009) 1337-1366.
[18] Bisi M., Martalò G. and Spiga G., *Acta Appl. Math.*, **132** (2014) 95-105.
[19] Madjarevic D., Ruggeri T. and Simic S., *Phys. Fluids*, **26** (2014) 106102.
[20] Grad H., *Commun. Pure Appl. Math.*, **5** (1952) 257-300.
[21] Salomons E. and Mareschal M., *Phys. Rev. Lett.*, **69** (1992) 269-272.
[22] Torrilhon M., *Annu. Rev. Fluid Mech.*, **48** (2016) 429-458.
[23] Torrilhon M. and Struchtrup H., *J. Fluid Mech.*, **513** (2004) 171-198
[24] Currò C. and Fusco D., *Atti Accad. Pelorit. Pericol., Cl. Sci. Fis. Mat. Nat.*, **91** (2013) 61-71.
[25] Grad H., *Commun. Pure Appl. Math.*, **2** (1949) 331-407.
[26] Kogan A. M., *J. Appl. Math. Mech.*, **29** (1965) 103-142.
[27] Levermore C. D., *J. Stat. Phys.*, **83** (1996) 1021-1065.
[28] Struchtrup, H., *Macroscopic Transport Equations for Rarefied Gas Flows* (Springer, Berlin Heidelberg New York) 2005.
[29] Brown S., Roe P. and Groth C., *in 12th Comput. Fluid Dyn. Conf.*, (1995) 337-351.
[30] Ohr Y. G., *Bull. Korean Chem. Soc.*, **17** (1996) 385-390.
[31] Suzuki Y. Yamamoto S. Van Leer B. and Boyd I. D., *in Computational Fluid Dynamics 2004* (Springer, Berlin Heidelberg New York) 2006, p. 529-534.
[32] Weiss W., *Phys. Rev. E*, **52** (1995) R5760.
[33] Bisi M., Groppi M. and Martalò G. , *Ric. di Mat.*, **-** (2020) 1-16. DOI: https://doi.org/10.1007/s11587-020-00503-x.
[34] Kestin J., Knierim K., Mason E. A., Najafi B., Ro S. T. and Waldman M., *J. Phys. Chem. Ref. Data*, **13** (1984) 229-303.
[35] Dyer T. M., *SAE Trans.*, **88** (1979) 790267-790526.
[36] Jaree A., Budman H., Hudgins R. R., Silveston P. L., Yakhnin V. and Menzinger M., *Catal. Today*, **69** (2001) 137-146.